Dust Particle Motion in the Vicinity of Dust Acoustic Waves

Edward Thomas, Jr. and Robert L. Merlino

Abstract—**In dc glow discharge dusty plasmas, the formation of dust acoustic waves is a commonly observed phenomenon. Experiments in the dusty plasma experiment device produce naturally occurring dust acoustic waves with frequencies $f \sim 5$ to 25 Hz and phase velocities of $v_{ph} \sim 0.5$ to 10 cm/s. Through the use of particle image velocimetry techniques, particle motion in the vicinity of the wavefronts is identified and measured. Particles are shown to have an oscillatory behavior near the dust acoustic wavefronts with peak speeds $v_{\max} \sim 4$ to 5 cm/s. Measurements are performed in argon dc glow discharge plasmas at pressures ranging from 90 to 120 mtorr. This paper discusses the correlation between the dust particle velocities and the density of dust particles in the vicinity of the wavefronts. The experimental measurements are compared against a linearized one-dimensional model for the waves. A brief discussion on the possible impact of nonlinear effects on the dust acoustic waves is also presented.**

Index Terms—**Dust acoustic wave, dusty plasma, glow discharge, particle image velocimetry, PIV.**

I. Introduction

SINCE Rao *et al.* [1], first postulated the existence of dust-driven collective modes, a great deal of effort has been put forth to classify wave behavior in dusty plasmas. Experiments [2]–[4], and theory [5]–[7], have identified a variety of wave modes in dusty plasmas. Nonetheless, questions still remain regarding the behavior of these collective modes in plasma. Specifically, much debate remains regarding the most appropriate method by which to model the behavior of the collective modes: Fluid models as compared against particle models. Additionally, there are questions about the mechanisms that provide the free energy to generate the waves in the plasma [1], [8].

A new measurement of dust particle motion in the vicinity of dust acoustic waves in a dc glow discharge dusty plasma is described.

Specifically, the oscillatory motion of dust particles at the wavefronts of dust acoustic waves is identified. The particle motion is shown to be generally correlated to the fluctuations in the dust particle density. A linear one-dimensional model for the perturbed motion of the dust particles is used to compare against the experimental measurements.

Manuscript received July 6, 2000; revised January 12, 2001. The work of E. Thomas, Jr., was supported by the National Science Foundation under Grant PHY-9733554. The work of R. L. Merlino was supported by the National Science Foundation under Grant PHY-9601041.

E. Thomas Jr., is with the Department of Physics, Auburn University, Auburn University, AL 36849–5311 USA (E-mail: etjr@physics.auburn.edu).

R. L. Merlino is with the Department of Physics and Astronomy, University of Iowa, Iowa City, IA 52242–1479 USA.

Publisher Item Identifier S 0093-3813(01)03688-8.

TABLE I
EXPERIMENTAL PARAMETERS FOR THE DUSTY PLASMA EXPERIMENT

Plasma Parameters:	
Gas	argon ($m_i = 40$ amu)
Pressure	$p = 90$ – 150 mTorr
Density	$n_e \approx n_i \sim 10^{15}$ m^{-3}
Electron temperature	$T_e = 2 - 4$ eV
Ion temperature	$T_i = 0.025$ eV
Dust Parameters:	
Dust particles	silica (SiO_2)
Dust diameter	$d_d \sim 40$ μm or 2.9 μm
Dust density	$N_d \sim 10^8 - 10^{10}$ m^{-3}

In this paper, the experimental hardware and diagnostics are first described. This is followed by a discussion of the experimental measurements of dust particle motion. Finally, a comparison is made between the experiment and the model.

II. Experimental Hardware

Experiments are performed on the dusty plasma experiment (DPX) device. The DPX device produces argon dc glow discharge plasmas using both a biased anode ($V_A = 190$ to 240 V) and a biased cathode ($V_C = 0$ to -130 V). Plasma parameters measured in the DPX device are typical for dc glow discharge plasmas. These parameters are listed in Table I. The ion (n_i) and electron (n_e) densities are quoted in the absence of dust particles in the plasma.

The source of the dust is a 2.5 cm × 2.5 cm tray located 3 cm below the anode. The dust particles are generally confined in the region between the anode and the tray. This is shown in Fig. 1. More detailed information on the operation of the DPX device is given elsewhere [9], [10].

III. Measurements

Dust acoustic waves (DAWs) are spontaneously generated in the DPX device. The wavefronts are propagating in the $-\hat{y}$ direction (i.e., downward in Fig. 1), away from the anode. In these experiments, dust acoustic waves have frequencies ranging $f_{DA} \sim 5$ to 25 Hz with wavelengths $\lambda_{DA} \sim 0.1$ to 0.5 cm. This yields phase velocities $v_{ph} \sim 0.5$ to 10 cm/s. These parameters are consistent with measurements in other experiments [3], [4].

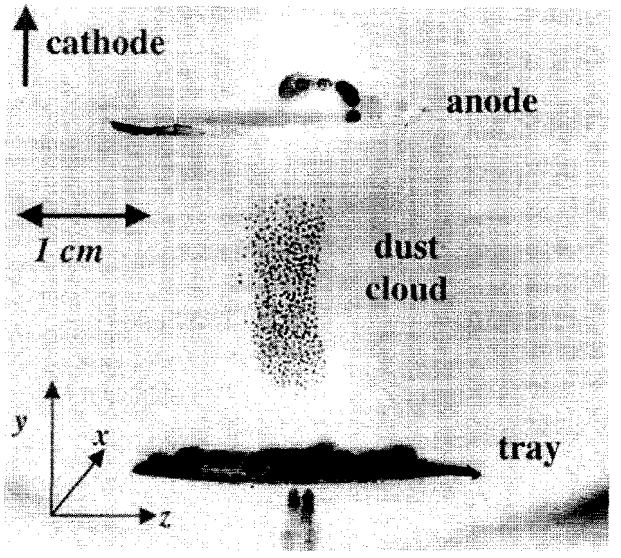

Fig. 1. Inverted image of a dust cloud suspended in the DPX device. A dust cloud of ~40 μm diameter silica particles is suspended in the plasma between the anode and the tray. All of the dusty plasmas discussed in this paper are formed in this region.

Particle image velocimetry (PIV) is used to measure the transport of the dust particles in the plasma. In the PIV technique, a pair of laser pulses, expanded into a two-dimensional (2-D) sheet by a cylindrical lens and separated in time by a user-defined separation, Δt_{laser} illuminates the dust cloud. The separation time between the two laser pulse ranges $0.4\ \mu\text{s} \leq \Delta t_{\text{laser}} \leq 30$ ms. A charge coupled devices (CCD) camera that is oriented perpendicularly to the light sheet captures the light scattered by the dust particles during each illumination. From the displacement of the dust particles between the two illuminations, a complete 2-D velocity profile can be reconstructed. It is important to note that the measured particle velocities represent an average over a several particles [9].

In the previously reported studies, measurements of the velocity profiles were obtained using separation times of $\Delta t_{\text{laser}} \sim 15$ to 20 ms [9], [10]. In order to obtain the measurements described in this paper, the separation time between the laser pulses is reduced to $\Delta t_{\text{laser}} \sim 1$ to 1.5 ms. This shorter separation time allows the particle motion along the wavefronts to be identified independently of the drift velocity of the entire wave structure.

A reconstruction of the velocity vectors of the dust particles along the wavefronts is shown Fig. 2. These measurements are performed at neutral pressures of $p = 100$ mtorr [in Fig. 2(a)] and $p = 120$ mtorr [in Fig. 2(b)]. In this series of experiments, the anode bias voltage is $V_A = 229$ V and the cathode bias voltage is $V_C = -95$ V. The source of dust particles is a silica powder with particles whose diameters range from $5\ \mu\text{m} \leq d \leq 40\ \mu\text{m}$.

It is observed that the velocity vectors generally lie along the wavefronts. The vectors show the dust particles to be oscillating in the vicinity of the wavefronts. The maximum particle speeds are $v_{\max} \sim 40$ mm/s.

In each image captured by the CCD camera, three quantities can be determined: the x and y locations of the dust grains and the intensity of the light scattered by the dust grain. The light intensity, I, is recorded as a 256-level grayscale value. In the inverted images shown in this paper, a bright spot (i.e., a black point) is represented by $I = 256$ and a dark spot (i.e., a white point) is represented by $I = 0$. By analyzing a vertical region through the dust cloud, it is possible to investigate the relationship between the particle motion and the location of the wavefronts.

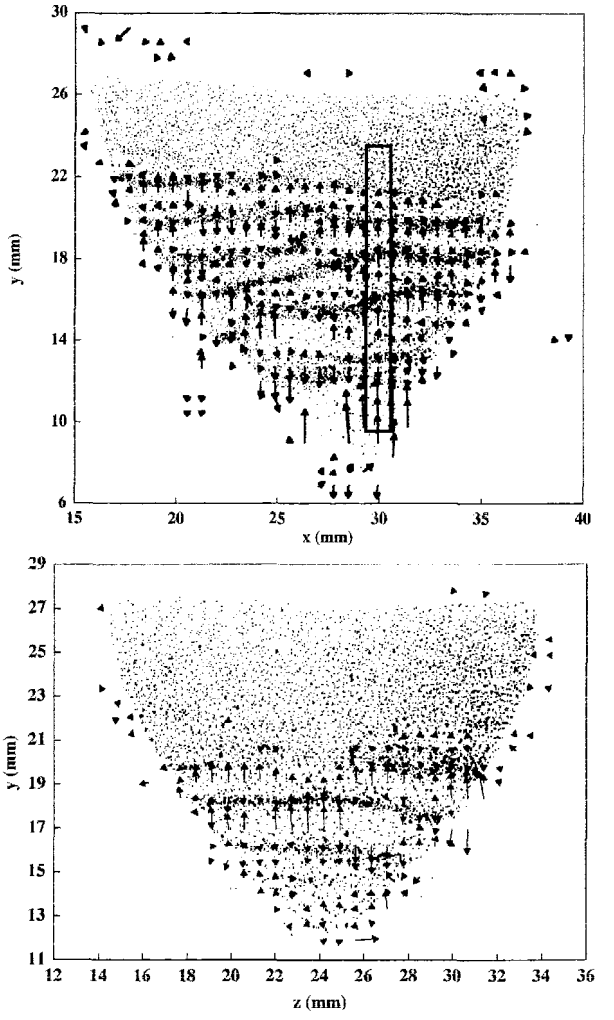

Fig. 2. 2-D velocity profile obtained using the PIV diagnostic system. The arrows represent the velocity vectors of the dust particles. It is observed that the vectors generally lie along the wavefronts. The anode bias voltage is $V_A = 229$ V and the cathode bias voltage is $V_C = -95$ V. Each image represents a different pressure. (a) $p = 100$ mtorr, and (b) $p = 120$ mtorr. In (a), a vertical interrogation region centered at $z = 29.93$ mm is identified by the black rectangle.

A vertical interrogation region for the 100 mtorr case is shown in Fig. 2(a). This region is 32 pixels wide ($\Delta z = 1.44$ mm) by 232 pixels high ($\Delta y = 10.44$ mm) and is centered at $z = 29.93$ mm. The width of this interrogation region coincides with the width of the analysis region used to reconstruct the velocity profiles. Along each row of pixels (i.e., for each vertical position y_k), the light intensity I_k is determined by averaging the light levels of the 32 pixels. This process is shown schematically in Fig. 3.

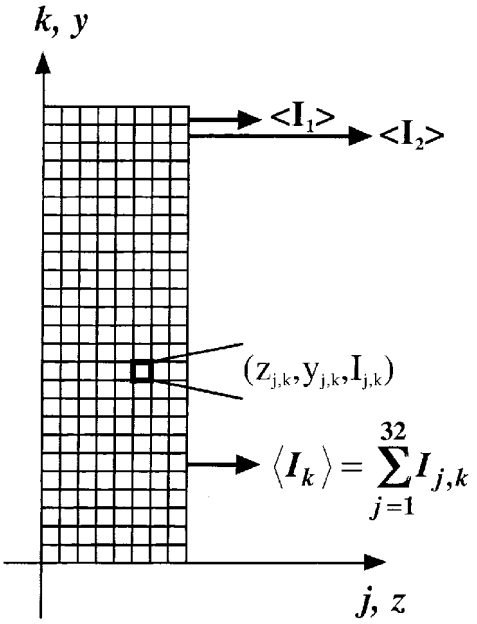

Fig. 3. Process for determining the average light intensity along the vertical interrogation region. The vertical interrogation region is divided into a grid of $j_{\max} \times k_{\max}$ pixels wide, where $j_{\max} = 32$ pixels and $k_{\max} \geq 200$ pixels. Each pixel location is identified by a horizontal position, $z_{j,k}$, a vertical position, $y_{j,k}$, and a light intensity, $I_{j,k}$. The average light intensity along a fixed vertical position in then determined by $\langle I_k \rangle = 1/32 \sum_{j=1}^{32} I_{j,k}$.

The relationship between the light intensity and dust particle density is complex. To completely unfold the density, detailed knowledge of the particle shapes, number of scattering objects, and the reflectivity of the dust particles is required [11]. Nevertheless, the intensity I_k can serve as an indicator of dust density fluctuations in the vicinity of the dust acoustic waves.

IV. Analysis and Discussion

A comparison of the particle velocities and the light intensity measurements is shown in Fig. 4 for the $p = 100$ mtorr case indicated in Fig. 2(a). The squares indicate the vertical component of the particle velocities (v_y) along a fixed z position (i.e., for the vertical interrogation region) as measured by the PIV diagnostic. The thin lines represent the light intensity I_k [or $I(y)$] over the same range. Measurements are made along the vertical line centered at $z = 29.93$ mm.

The figure shows an oscillation in the light intensity level for 13 mm $\leq y \leq$ 23 mm. This corresponds to the visible increase and decrease of the dust particle density along the wavefronts of the dust acoustic waves. The spacing between the peaks gives a measurement of the wavelength. The average wavelength is $\langle \lambda \rangle \approx 2.25 \pm 0.65$ mm.

The thick curve that passes through the velocity measurements is a sinusoidal curve fit to the velocity of the form: $v_y = v_{0y} \sin(\mathrm{k_y y} - \varphi)$, where v_y is the particle velocity, v_{0y} is the amplitude of the oscillation (in mm/s), k_y is the wave number (in mm^{-1}), and φ is a phase. The fit in for Fig. 4 is given by: $v_y = 47 \sin(2.1\mathrm{y} + 2.32)$ mm/s. This fit corresponds to a dust acoustic wavelength of $\lambda \approx 2.9$ mm.

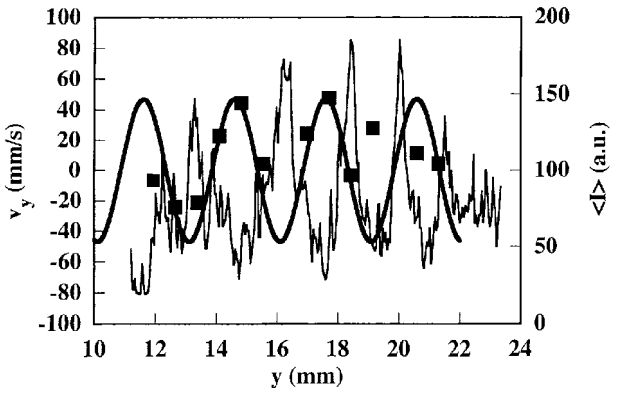

Fig. 4. Comparison of the dust particle velocities and light intensity measurements along a vertical interrogation. Measurements are shown for the experiment performed at $p = 100$ mtorr, as indicated in Fig. 3(a). The squares indicate the vertical component (v_I) of the particle velocities along a vertical line at $z = 29.93$ mm. The thin lines represent the light intensity $\langle I \rangle$ over the same vertical region. The thick curve that passes through the velocity measurements is a sinusoidal curve fit to the velocity. The equation of the curve fit is given by: $v_y = 47 \sin(2.1y + 2.32)$ mm/s.

In the usual analysis of wave motion, the one-dimensional continuity equation is linearized to obtain the relationship between the plasma density and the phase velocity of the wave. Here n is the dust particle density and v is the dust particle velocity

$$\frac{\partial n}{\partial t} + \frac{\partial}{\partial x}(nv) = 0. \tag{1}$$

The density and velocity are assumed to vary in time and space according to $a_0 + a_1 e^{i(ky+\omega t)}$ where the zeroth-order terms are constants and the first-order terms are the perturbed quantities and the wave is assumed to be propagating in the $-y$ direction. Using this assumption, the linearized form of (1) becomes:

$$i\omega n_1 + ikn_0 v_1 + ikn_1 v_0 = 0. \tag{2}$$

Furthermore, if the unperturbed velocity of the dust particles is assumed to be $v_0 \sim 0$ m/s, then (2) can be rewritten as

$$\left(\frac{n_1}{n_0}\right) = -\left(\frac{v_1}{v_{ph}}\right) \tag{3}$$

where $v_{ph} = \omega/k$.

In this one-dimensional (1–D) approach, the ratio of the phase velocity of the wave to the perturbed velocity of the particles is compared with the ratio of the unperturbed density to the perturbed density. The experimental measurement of the velocity vectors along the wavefronts is interpreted as the perturbed velocity component, v_1.

The average value of the light intensity $\langle I \rangle$ through a vertical region is used as n_0. This is computed from the arithmetic mean of the light intensity measurements along a vertical interrogation region. The estimate of the value of n_1 is determined by the following process: the median value of the light intensity (I_{med}) is computed along the vertical interrogation region; this I_{med} represents the background light intensity. The amplitude of the density fluctuation, n_i is then computed from (1/2) of

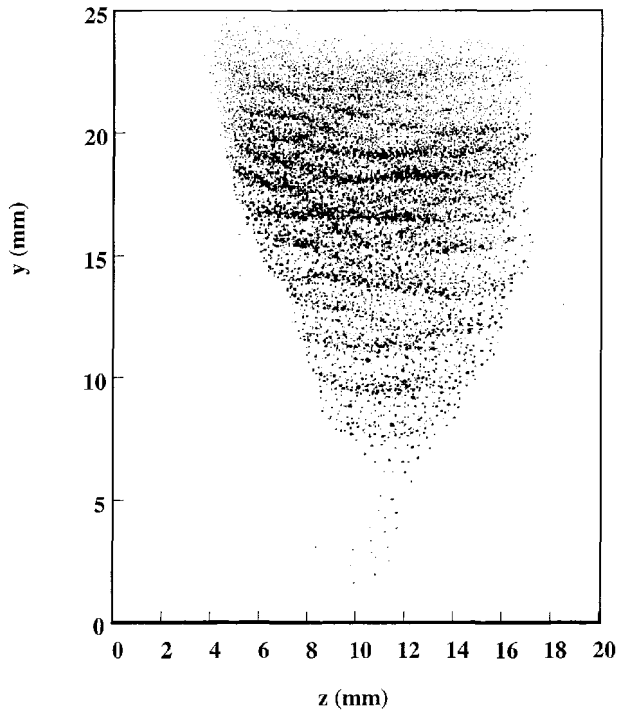

Fig. 5. Inverted image of a dust cloud of 2.9-μm diameter spherical silica particles in the DPX device. Note that this dust cloud has generally the same shape as compared to the dust cloud formed using the 40-μm diameter particles. However, with the 2.9-μm particles, the dust acoustic waves appear to propagate along the entire vertical length of the dust cloud.

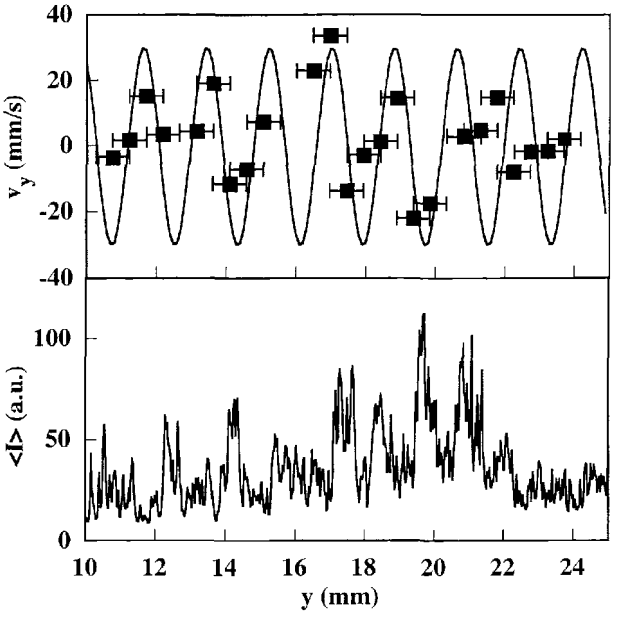

Fig. 6. Comparison of the dust particle velocities and light intensity measurements along a vertical interrogation region. In the upper plot, the squares indicate the vertical component of the particle velocities (v_y) along a vertical line centered at $z = 13.86$. The solid line is a sinusoidal curve fit and is given by: $v_y = -30\sin(3.5\mathrm{y} + 1.80)$ mm/s. The thin lines in the lower plot represent the light intensity $\langle I \rangle$ over the same vertical region.

the difference between the maximum peak in the intensity and I_{med}, $n_1 = 1/2(I_{\max} - I_{\mathrm{med}})$. When these measurements are combined, with the experimental measurement of the phase velocity, v_{ph}, it is possible to compute the ratios indicated in (3).

To test the validity of approach, a second experiment is performed. In this second experiment, a new source of dust particles is used. These particles are spherical silica particles with a normal distribution of particles sizes with an average diameter of $d = 2.9 \pm 0.8$ μm. A photograph of a dust cloud made in an argon plasma with V_A =206 V, $V_C = -132$ V, and p =120 mtorr is shown in Fig. 5. It is observed that the dust cloud of 2.9-μm particles has generally the same shape as the dust cloud using the 40-μm particles. The primary difference is that the dust acoustic wavefronts appear to extend throughout the entire vertical length dust cloud with the 2.9-μm particles as compared to just the lower section of the clouds with the 40-μm particles as shown in Fig. 2.

A comparison of the particle velocities and the light intensity measurements is shown in Fig. 6 for the cloud shown in Fig. 5 along the vertical line centered at z =13.86 mm. In upper plot, the squares indicate the vertical component of the particle velocities (v_y) along the fixed z position as measured by the PIV diagnostic. The solid line is a sinusoidal curve fit and is given by: $v_y = -30\sin(3.5\mathrm{y} + 1.80)$ mm/s. This fit corresponds to a dust acoustic wavelength of $\lambda \approx$1.8 mm. In the lower plot, the thin lines represent the average light intensity $\langle I \rangle$ over the same range. The magnitude of the particle speed and the wavelength are comparable to those measured using the 40 μm particles.

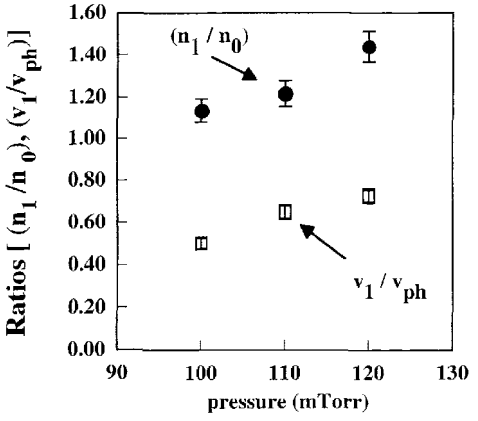

Fig. 7. Comparison of the ratios $|v_1/v_{ph}|$ (shown as the open squares) and $|I_{\max}/\langle I \rangle|$ (shown as the closed circles) at pressures ranging from 90 to 120 mtorr. The error in these measurements is estimated at $\sim$10%.

However, the peaks in the light intensity measurement are considerably lower, possibly suggesting a smaller variation in the dust particle density that in the previous experiments.

Measurements of dust acoustic waves in dust clouds composed of the 2.9-μm diameter particles are made at neutral pressures of 100, 110, and 120 mtorr. The anode bias voltage and the cathode bias voltage are fixed at V_A =206 V and $V_C = -132$ V, respectively. In each case, a comparison of $|v_1/v_{ph}|$ and $|n_1/n_0|$ is made. The results of these comparisons are shown in Fig. 7. It is observed that the ratio of $|v_1/v_{ph}| \sim 0.5$ to 0.8, and the ratio $|n_1/n_0| \sim 1.2$. While it must be noted that the light intensity measurements are not a direct measurement for the density, both the intensity measurement and the video images of

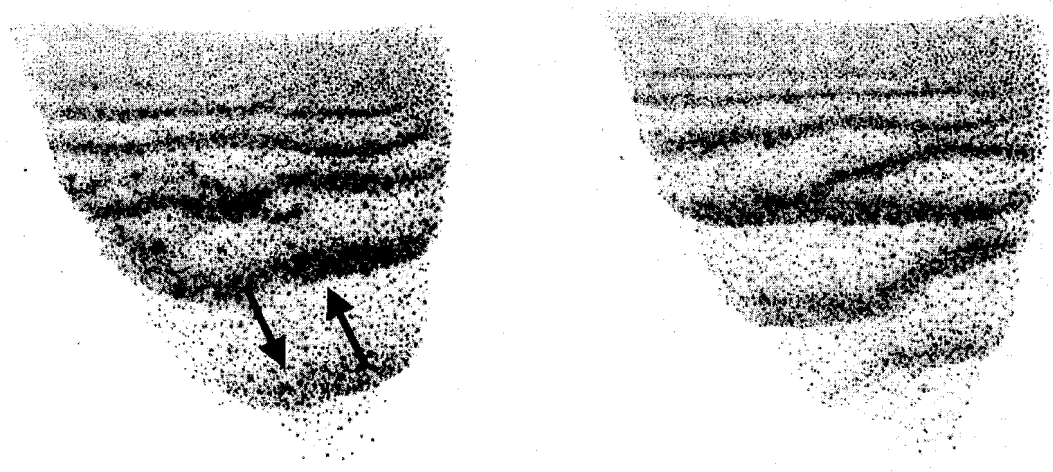

Fig. 8. Reflection of a dust acoustic wave near the bottom of the dust cloud is shown. In the image on the right, the motion of two wavefronts is indicated by the two arrows. In the image on the left, which is taken $\Delta t = 120$ ms after the first image, the resulting wavefronts are shown.

the dust clouds do suggest that there is a substantial increase in the dust particle density along the wavefronts. The disagreement between the two ratios suggests that there are physical factors present in the experiment that cause the waves to deviate from the linear theory.

One of these factors is the fact that the waves are not completely planar. This is most likely due to the shape of the dust clouds produced in the DPX device. This effect can be clearly seen in Fig. 2. This effect of the shape of the dust cloud on the properties of the waves has been observed in other dusty plasma experiments [2], [12]. Another factor that may modify the propagation of the waves is reflection. The waves generally propagate downward, away from the anode to the bottom of the dust cloud. Once reaching the bottom, a portion of the wave is occasionally observed to reflect from the bottom of the cloud and propagate upward. This effect is most prominent at the operating lower pressures and is shown in Fig. 8 for the 40 μm diameter particles at a pressure of $p = 90$ mtorr.

Additionally, the dust grains used in this experiment are not uniform in shape or size. This would allow the grains to accumulate slightly different amounts of charge. It has been proposed that these charge differences could lead to the formation of nonlinear dust acoustic waves [13], [14]. However, there is limited theoretical guidance for exploring nonlinear effects on dust acoustic waves and considerably more experimental and theoretical work is needed to confirm the existence of nonlinear effects.

In summary, this paper describes experimental measurements of dust particle oscillations in the vicinity of dust acoustic waves. The dust particles are observed to oscillate with peak speeds $v_1 \sim 20$ to 40 mm/s. While there is a correlation between the oscillations in the dust density and dust particle velocity, analysis of the wave behavior suggests that the wave motion deviates from a linear theory. However, it should be noted that results of this study further suggest that the use of the light intensity fluctuations may not be the ideal method by which to characterize the variation of the dust density. Nonetheless, these measurements do highlight the flexibility of the PIV technique in making measurements in dusty plasmas.

ACKNOWLEDGMENT

E. Thomas, Jr. would like to acknowledge the NASA-Fisk University Center for Photonic Materials and Devices, Nashville, TN, where several of the initial measurements in this study were performed.

REFERENCES

[1] N. N. Rao, P. K. Shukla, and M. Y. Yu, "Dust acoustic waves in dusty plasmas," *Planet. Space Sci.*, vol. 38, p. 543, 1990.
[2] A. Barkan, R. L. Merlino, and N. D'Angelo, "Laboratory observation of the dust-acoustic wave mode," *Phys. Plasmas*, vol. 2, p. 3563, 1995.
[3] R. Merlino, A. Barkan, C. Thompson, and N. D'Angelo, "Laboratory studies of waves and instabilities in dusty plasmas," *Phys. Plasmas*, vol. 5, p. 1607, 1998.
[4] H. R. Prabhakara and V. L. Tanna, "Trapping of dust and dust acoustic waves in laboratory plasmas," *Phys. Plasmas*, vol. 3, p. 3176, 1996.
[5] B. S. Xie, K. F. He, Z. Q. Huang, and M. Y. Yu, "Dust shielding and correlation function for dusty plasmas," *Phys. Plasmas*, vol. 6, p. 2997, 1999.
[6] M. Rosenberg and G. Kalman, "Dust acoustic waves in strongly coupled dusty plasmas," *Phys. Rev. E, Stat. Phys. Plasmas Fluids Relat. Interdiscip. Top.*, vol. 56, p. 7166, 1997.
[7] X. Wang and A. Bhattacharjee, "Hydrodynamic waves and correlation functions in dusty plasmas," *Phys. Plasmas*, vol. 4, p. 3759, 1997.
[8] M. Rosenberg, "Ion-dust streaming instability in processing plasmas," *J. Vac. Sci. Technol. A, Vac Surf. Films*, vol. 14, p. 631, 1996.
[9] E. Thomas Jr., "Direct measurements of two-dimensional velocity profiles in direct current glow discharge dusty plasmas," *Phys. Plasmas*, vol. 6, p. 2672, 1999.
[10] E. Thomas Jr. and M. Watson, "First experiments in the Dusty Plasma Experiment device," *Phys. Plasmas*, vol. 6, p. 4111, 1999.
[11] C. Hollenstein, J.-L. Dorier, J. Dutta, L. Sansonnens, and A. A. Howling, "Diagnostics of particle genesis and growth in RF silane plasmas by ion mass spectrometry and light scattering," *Plasma Sources Sci. Technol.*, vol. 3, p. 278, 1994.
[12] C. Thompson, A. Barkan, N. D'Angelo, and R. L. Merlino, "Dust acoustic waves in direct current glow discharge," *Phys. Plasmas*, vol. 4, p. 2331, 1997.

[13] S. V. Singh and N. N. Rao, "Linear and nonlinear dust-acoustic waves in inhomogeneous dusty plasmas," *Phys. Plasmas*, vol. 5, p. 94, 1998.
[14] ——, "Effect of dust charge inhomogeneity on linear and nonlinear dust-acoustic wave propagation," *Phys. Plasmas*, vol. 6, p. 3157, 1999.

Edward Thomas, Jr. was born on St. Thomas, U.S. Virgin Islands, in 1968. He received the B.S. degree from the Florida Institute of Technology, Melbourne, FL, the M.S. degree from MIT, Cambridge, MA, and the Ph.D. degree from Auburn University, Auburn University, AL, in 1989, 1993, and 1996, respectively. His graduate studies focused on particle transport in fusion energy experiments.

In 1996, he joined the faculty of Fisk University, Nashville, TN, where he established a new plasma physics laboratory. In 2000, he returned to Auburn University as an Assistant Professor of physics, where he has established a laboratory for the study of basic plasma science. He currently maintains two independent research projects: an experiment on the growth and suppression of plasma instabilities in the presence of rotating plasmas and an experiment on particle transport and dust grain charging in dusty plasmas.

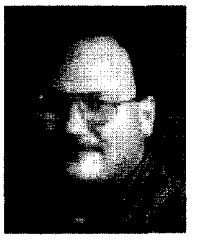

Robert L. Merlino was born in Philadelphia, PA in 1951. He received the B.S. degree in physics from St. Joseph's College, Philadelphia, PA, and the Ph.D. degree in physics from the University in Maryland, College Park, in 1973 and 1980, respectively.

From 1980 to 1981 he was a Postdoctoral Research Scientist at the Plasma Physics Laboratory, Columbia University, New York. In 1981, he joined the Department of Physics and Astronomy, University of Iowa, Iowa City, where he is currently a Professor. He has been involved in basic plasma physics experiments investigating phenomena with space plasma physics applications. Over the last several years, he has concentrated on experimental investigations of the behavior of dusty plasmas, with particular emphasis on waves and instabilities in dusty plasmas. He, along with John Goree and Amitava Bhattacharjee, are organizing the 9th Workshop on the Physics of Dusty Plasmas, to be held in Iowa City, IA, in May 2001.

Dr. Merlino has been chosen as a Distinguished Lecturer in Plasma Physics by the American Physical Society Division of Plasma Physics for the academic year 2000–2001.